Relationship between velocity and anisotropy perturbations and anomalous stress field around salt bodies

MITA SENGUPTA, RAN BACHRACH, and ANDREY BAKULIN, WesternGeco/Schlumberger

Downloaded 01/02/23 to 73.136.105.228. Redistribution subject to SEG license or copyright; see Terms of Use at http://library.seg.org/page/policies/terms
DOI:10.1190/1.3124936

Due to a growing demand for new hydrocarbon reservoirs, subsalt exploration has increased significantly during this decade. Subsalt imaging and drilling pose many challenges and opportunities, and subsalt velocity estimation is crucial for both tasks.

In recent years, many efforts have been dedicated to improve subsalt imaging. Examples include better velocity models, more accurate migration algorithms, multiple attenuation, and improved illumination with wide-azimuth seismic data acquisition. Velocity estimation is required for imaging around salt bodies and for drilling hazard identification. A common practical approach for subsalt velocity modeling is to perform a subsalt interpretation, and then superimpose a regional velocity gradient below the salt as an initial velocity estimate. From a rock physics standpoint, using a regional velocity versus depth estimate ignores the facts that:

- velocities are related to effective stress and not depth of the sediment
- the presence of complex salt bodies can give rise to anomalous 3D stresses in the subsurface, which can perturb subsurface velocity and anisotropy

Subsalt velocity analysis is a challenging task, as the seismic signature below salt is often weak, making it difficult to pick reliable moveout of events, which is required for any velocity estimation. Therefore, additional information related to the physical processes associated with salt bodies should improve our ability to constrain velocity models in poor-data areas typically associated with the near-salt and subsalt environment. In this study, we use geomechanics to provide such constraints.

Salt, being less dense than surrounding sediments, gives rise to large buoyant forces, leading to significant reduction in subsalt stresses. Using a simple 1D approach, vertical stress can be estimated by integrating the density of the formation column. We expect the average vertical stress to be smaller for a section containing a salt body than for one without it. Thus, velocities below salt would be generally lower because the vertical stress is lower. Existing approaches perform one-dimensional updates of subsalt velocities using vertical effective stress. However, all these 1D approaches are overly simplistic, and the actual 3D stress state in the presence of irregular and rugose salt bodies may be much more complex. It has been shown that 3D modeling of the stress field with actual salt geometry can appropriately describe large stress perturbations near salt bodies (Fredrich et al., 2003). Over the last few years, members of the drilling community used geomechanical analyses to study subsurface stress distributions to identify drilling hazards, zones of instability, and reduced fracture gradient close to salt diapirs. Bakulin et al. (2008) presented a field example where anomalous ratio between horizontal and vertical effective stress leads to abnormal V_S-V_P relationships subsalt. This study suggests that the ability to predict vertical and horizontal stresses is also crucial to better characterize the effects of salt-induced stresses on the sediment petrophysical properties.

The relation between stress perturbation and seismic velocity has been studied extensively. Both experimental and theoretical studies have shown that stresses and strains affect velocity. Reduction in effective stresses leads to velocity reduction, and anisotropic stresses lead to anisotropic velocities. Seismic data span a range of propagation angles, and while vertical stress may control vertical velocity, near-vertical propagation is greatly affected by horizontal stresses (Sarkar et al., 2003). The ability to link the state of stress in the subsurface to the expected velocity can serve as a powerful tool in our quest to estimate subsalt velocities.

In this paper, we apply 3D geomechanical modeling to a real and complex salt structure and its surrounding sedimentary rock. Unlike many published geomechanical analyses of salt bodies, which have been confined to idealized salt geometries, we use a real 3D salt model obtained from an actual wide-azimuth survey in the Gulf of Mexico (Howard, 2007). We derive the salt geometry from 3D seismic, model stress and strain perturbations associated with the presence of salt, and transform the modeled perturbation into an updated anisotropic velocity model using a rock physics transform based on nonlinear elasticity. We show that the presence of a complex salt body within a sedimentary basin can cause large stress perturbations in the surrounding rock, which in turn can lead to large velocity reductions below salt and significant velocity anisotropy adjacent to the salt flanks.

Review of background theory

Rock physics transforms between 3D stress and anisotropic velocity. Let us consider a rock that can be described by vertical transverse isotropy (VTI) in a reference state. For the simplest unstressed state, Hooke's law for VTI rock defines a linear relationship between stresses σ_{ij} and strains e_{kl}. Coefficients of proportionality are represented by a stiffness tensor C^0_{ij}, which has only five independent moduli for VTI rock. To describe seismic signatures, it is convenient to characterize the same rock using different set of parameters: the vertical velocities of P-waves and S-waves (V_{P0} and V_{S0}) and three Thomsen parameters, ε_b, δ_b, γ_b (Tsvankin, 2005). For isotropic media these dimensionless anisotropy parameters all become zero, while nonzero values describe intrinsic anisotropy. Under applied stress, all elastic parameters change—generally increasing with increasing stress. The effective elastic stiffness, C_{ij}, defining seismic velocities under stress can be described by nonlinear elasticity (Prioul et al., 2004). Any stiffness un-

Downloaded 01/02/23 to 73.136.105.228. Redistribution subject to SEG license or copyright; see Terms of Use at http://library.seg.org/page/policies/terms
DOI:10.1190/1.3124936

der stress is equal to corresponding unstressed stiffness plus additional perturbation caused by each of the stress components. This transform has attractive simplicity in that stress perturbations are a product of nonlinear elastic constants and strains. Therefore these nonlinear constants can be thought of as stress sensitivity parameters. Nonlinear elasticity acts as a rock physics transform that allows prediction of the complete stiffness tensor under stress if we know only the unstressed stiffnesses and the applied stress tensor.

In the simplest case, nonlinear elasticity requires three third-order (nonlinear) elastic constants, c_{111}, c_{112}, and c_{123}, that describe stress sensitivity. For P-wave seismic signatures, it is also convenient to use an additional constant $c_{155}=(c_{111}-c_{112})/4$. Values of the nonlinear constants are reported in various studies (e.g., Sarkar et al.; Lebrat and Prioul, 2004). Stresses here are understood as effective stresses. It can be shown that, in this approximation, the effective stiffness tensor under stress is equivalent to an elastic orthorhombic material with some new modified stiffnesses dependent on strains or stresses.

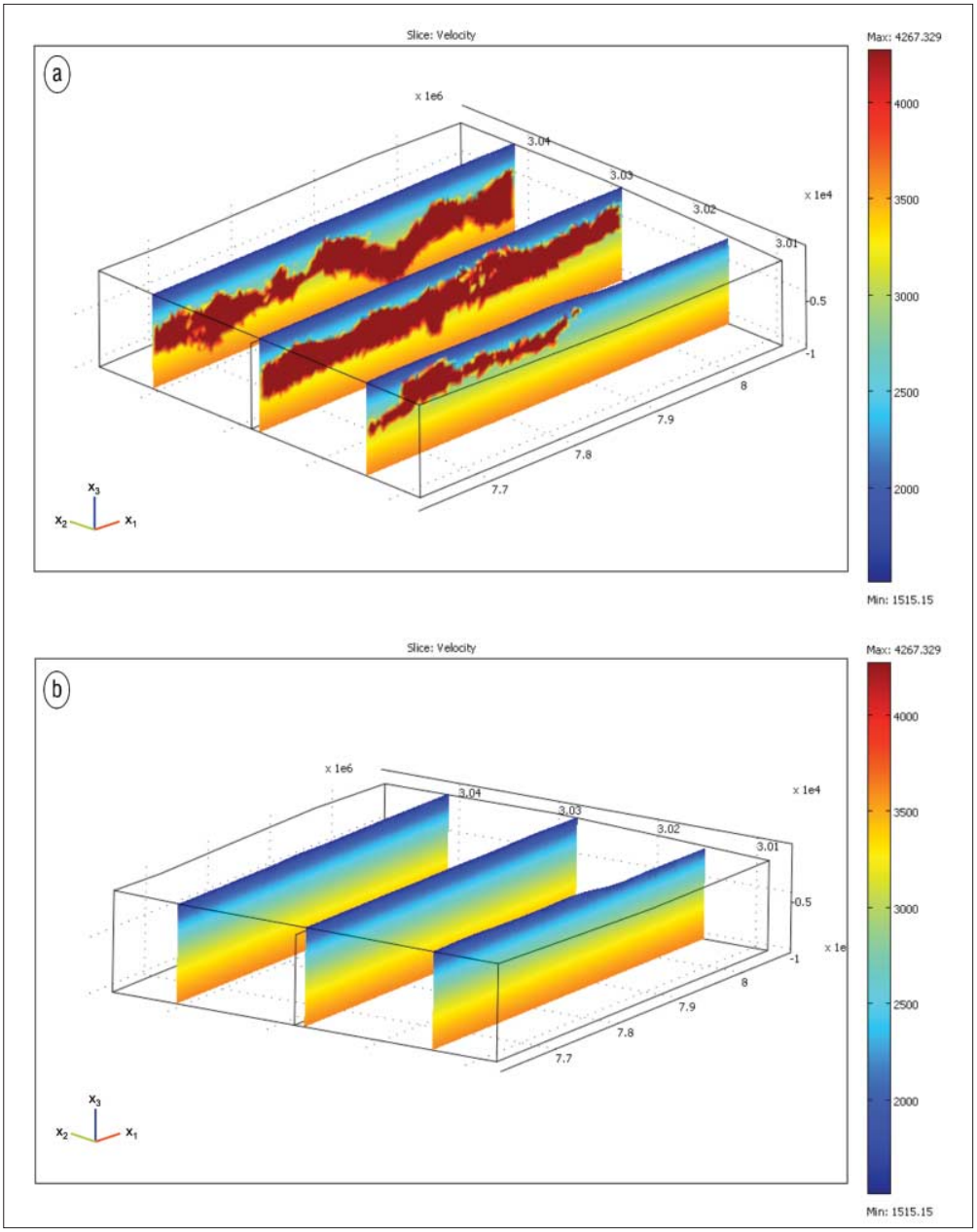

Figure 1. *Velocity slices through the two 3D models. (a) Sediment model with salt body; salt has higher velocity than sediments; (b) sediment-only reference model.*

Now that we have defined a complete rock physics transform between 3D stress and the full effective stiffness matrix of the rock under stress, we can predict velocity dependence for any arbitrary direction or estimate any seismic signature of interest if we know 3D stresses, initial stiffnesses of the rock in a reference state, and stress sensitivity parameters (third-order constants).

Quantifying stress anomalies. To apply the rock physics transform described above to the case at hand, we need to define an appropriate reference state. In practice we have good understanding of sediment elastic properties and subsurface stresses in open basins away from salt. Therefore it is convenient to take this state as a reference state. Then our objective would be to quantify perturbations in 3D stress caused by salt bodies and convert them into perturbations in seismic velocity and anisotropy. While this may not reflect the entire geologic history and evolution of the basins, we think it is a reasonable first-order approach for capturing the anomalous imprints of the entire 3D stress tensor as opposed to only vertical stress or pore pressure simulated in basin modeling.

Geomechanical modeling uses two different finite-element models. The first model consists of a salt body within a sedimentary basin. The second is a reference or background model that consists of sediments only without salt. Independent geomechanical computation in these two models, using the same boundary conditions, allows quantifying change in strains Δe and stresses $\Delta\sigma$ associated with the presence of salt by subtracting the total strain (stress) of the background

Downloaded 01/02/23 to 73.136.105.228. Redistribution subject to SEG license or copyright; see Terms of Use at http://library.seg.org/page/policies/terms
DOI:10.1190/1.3124936

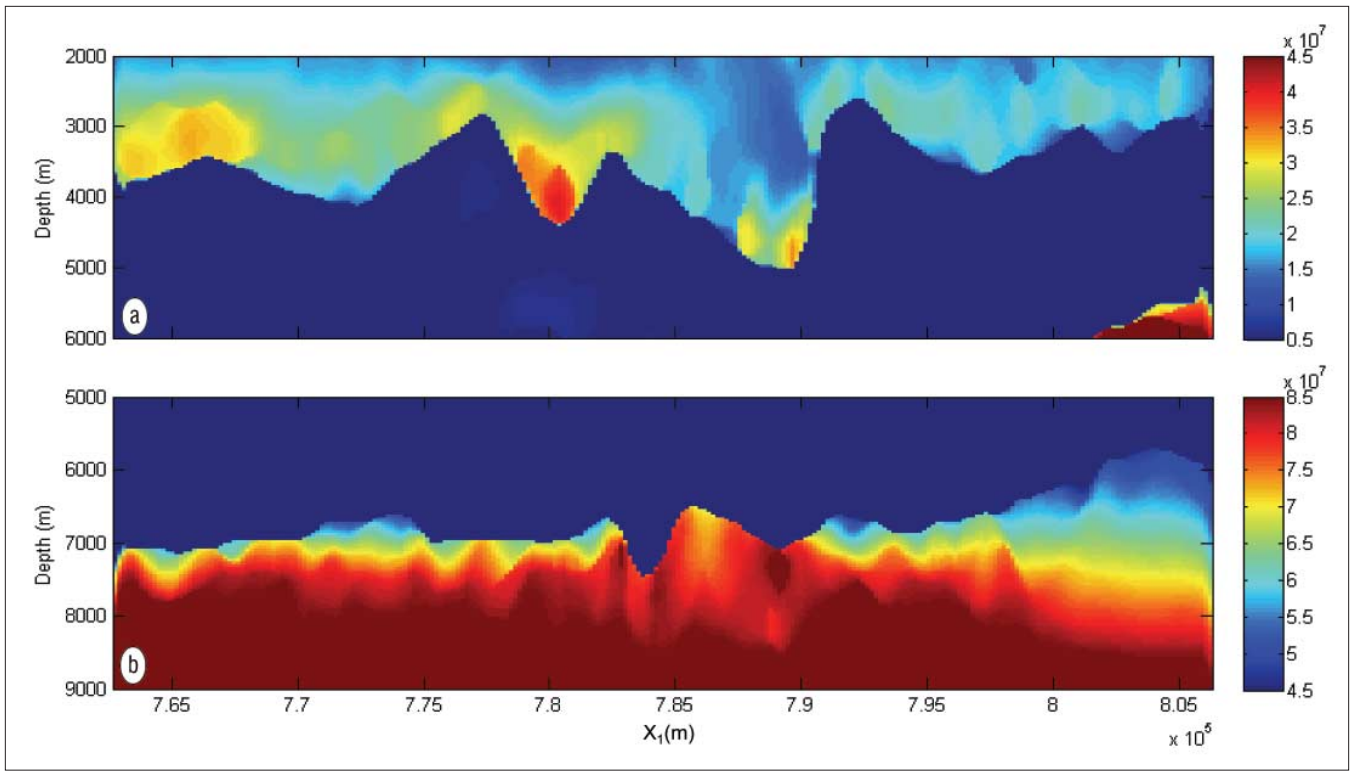

Figure 2. *Cross section of computed von Mises stress (a measure of deviatoric stress) through the 3D salt model: (a) above salt and (b) below salt. Note that the von Mises stress is high near the flanks of the salt body, and goes to zero inside the salt body or far away from salt. Rugose salt boundary introduces substantial spatial variation in von Mises stresses that is not present in sediment models without salt.*

model (e_{back}, σ_{back}) from the strain (stress) of the model with salt (e_{salt}, σ_{salt}):

$$\Delta e = e_{salt} - e_{back}, \Delta\sigma = \sigma_{salt} - \sigma_{back} \quad (1)$$

Δe and $\Delta\sigma$ represent the salt-induced 3D strain/stress distribution.

Assuming that the elastic properties of the sediments are known for a reference state, we can predict the modified stiffness tensor from the differential strains (Δe) by using equations of nonlinear elasticity. Knowledge of stress sensitivity parameters (nonlinear constants) is required. Knowing effective elastic tensor under stress, we can predict any other seismic signature of interest including velocity and anisotropy parameters required for imaging. Therefore we can aid subsalt velocity estimation by either directly using these predicted velocities if the rock physics transform is calibrated, or at least guiding a spatial variation of the velocities/anisotropies in a more qualitative fashion.

Gulf of Mexico example

In this section, we show an example from an area in the Gulf of Mexico containing a large and complex salt body. The salt geometry was obtained from a 3D seismic data set. The initial velocity model for the sediments was obtained from regional depth trends, although, in general, it can be obtained from other sources such as tomography and velocity profiles from nearby wells.

Geomechanical modeling. We modeled a large volume: 10-km deep and 30 × 40-km horizontally. We built two 3D heterogeneous finite-element models. The first model consists of one or more salt bodies within a sediment volume. The second model consists of a sediment volume without salt. To take into account the 3D spatial structure of the large and complex salt body, we used a large number of finite-element grids (about 100,000 elements), with refined grid spacing near the inline of interest. The physical properties of the two models are identical where there is no salt. The background model contains sediment-like properties corresponding to the salt locations. Figure 1 shows vertical slices through each of our finite-element models. Note that the sediment velocity and density increase with depth. Observe that the salt has higher velocity and lower density compared to the surrounding sediments.

Standard geomechanical modeling with salt diapirs simulates salt as a viscoelastic material with creep (Fredrich et al.). In our case, viscoelastic behavior of salt was approximated by a linearly elastic solid with a large Poisson's ratio of 0.495. To validate the assumption used for salt modeling, we tested this solution against a standard viscoelastic solution for simple salt geometries and smaller model sizes, and obtained similar results. Given the computational constraints existing for the large data set, and the details of the salt geometry, we believe that the approach of approximating the viscoelastic behavior of salt is a reasonable trade-off for the current purpose, which is velocity model building.

Stress-strain solutions. We observe that the salt geometry has a significant impact on the 3D distribution of stresses and

Downloaded 01/02/23 to 73.136.105.228. Redistribution subject to SEG license or copyright; see Terms of Use at http://library.seg.org/page/policies/terms
DOI:10.1190/1.3124936

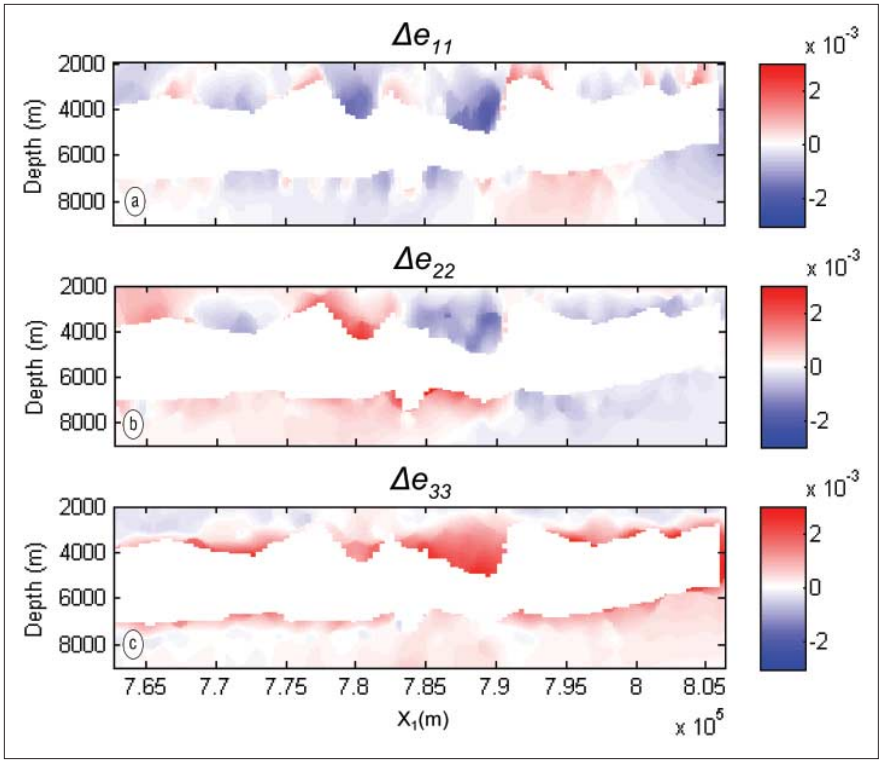

Figure 3. *Salt-induced or anomalous strains shown as a cross section through a 3D model: (a) horizontal strain along x_1-axis; (b) horizontal strain along x_2-axis; (c) vertical strain along x_3-axis. They are obtained by subtracting strains in the model with salt and reference model without salt. These differential strains are utilized to compute velocity and anisotropy perturbations caused by presences of salt. Unequal horizontal strains imply strain and stress anisotropy near salt flanks.*

strains. Figure 2 shows the von Mises stress derived from the finite-element modeling. The von Mises stress is defined as

$$\sigma_{VM} = \sqrt{\frac{(\sigma_1-\sigma_2)^2+(\sigma_2-\sigma_3)^2+(\sigma_3-\sigma_1)^2}{2}} \qquad (2)$$

where σ_1, σ_2, and σ_3 are the principal stresses. Von Mises stress is a scalar function of the stress tensor that gives an appreciation of the overall magnitude of the deviatoric stresses. The salt itself does not support shear stress, and therefore has zero deviatoric stresses inside it; but near the edges of the salt body, especially near the areas showing significant topography, we observe high and variable von Mises stresses and large stress anisotropy in sediments. For a general salt geometry, all stress components are expected to be nonzero. This means that principal stresses or strains are no longer aligned with the original coordinate axes. For simplicity, in this initial study we ignore small off-diagonal elements of the stress and strain tensors and do not quantify rotation of the stress field. Under this approximation, we are still able to use the simple equations of Prioul et al. as opposed to elaborate equations describing more complex symmetries that are at least tilted orthorhombic.

The strain difference (Δe), components of which are shown in Figure 3, are caused by the presence of the salt body; hence, we refer to them as the salt-induced strains. In the next section, we describe how we used a 3D stress-to-velocity transform based on nonlinear elasticity to compute the anisotropic velocity changes caused by the salt-induced strains.

Updating velocity and anisotropy. Once we have computed Δe throughout the 3D volume, we apply a rock physics transform based on nonlinear elasticity to compute the modified stiffness tensor under stress. For example, from the updated stiffness tensor (C_{ij}) and density (ρ), we compute velocities along the coordinate axes (x_1, x_2, x_3). A more convenient parameterization to describe reflection seismic signatures was given by Tsvankin (2005). If we are only interested in P-waves, then relevant parameters of the effective orthorhombic material are defined as P-wave vertical velocity (V_{P0}) and two pairs of Thomsen-style VTI parameters in two orthogonal vertical planes. Anisotropic wave propagation in the x_1, x_3 symmetry plane normal to the x_2 direction is controlled by the VTI parameters $\varepsilon^{(2)}$ and $\delta^{(2)}$. In this plane, $\varepsilon^{(2)}$ describes fractional difference between horizontal and vertical P-wave velocities, whereas $\delta^{(2)}$ describes the difference between NMO velocity and a vertical velocity according to the equation $V_{nmo}^{(2)} = V_{P0}\sqrt{1+2\delta^{(2)}}$. Likewise, anisotropic wave propagation in the x_2, x_3 symmetry plane normal to the x_1 direction is characterized by VTI parameters $\varepsilon^{(1)}$ and $\delta^{(1)}$. Similarly, in this plane, $\varepsilon^{(1)}$ describes fractional difference between horizontal and vertical P-wave velocities, whereas $\delta^{(1)}$ describes the difference between NMO velocity and a vertical velocity $V_{nmo}^{(1)} = V_{P0}\sqrt{1+2\delta^{(1)}}$.

In the weak-anisotropy limit, azimuthal variation of NMO velocity between two horizontal directions is controlled by the difference between δ in two vertical symmetry planes according to the equation

$$\frac{V_{nmo}^{(1)}-V_{nmo}^{(2)}}{V_{nmo}^{(1)}} \approx \delta^{(1)}-\delta^{(2)} \qquad (3)$$

To gain further insight between seismic signatures and 3D stress, it is convenient to apply the weak-anisotropy approximation and express values of anisotropic parameters as a function of stress (Sarkar et al.):

$$\varepsilon^{(1)} = \varepsilon_b + \frac{K_p}{2C_{55}^0}(\sigma_{22}-\sigma_{33}),\ \varepsilon^{(2)} = \varepsilon_b + \frac{K_p}{2C_{55}^0}(\sigma_{11}-\sigma_{33}) \qquad (4)$$

$$\delta^{(1)} = \delta_b + \frac{K_p}{2C_{55}^0}(\sigma_{22}-\sigma_{33}),\ \delta^{(2)} = \delta_b + \frac{K_p}{2C_{55}^0}(\sigma_{11}-\sigma_{33}) \qquad (5)$$

where

$$K_p = \frac{2c_{155}}{C_{33}^0}$$

is a single stress-sensitivity parameter that controls P-wave

Downloaded 01/02/23 to 73.136.105.228. Redistribution subject to SEG license or copyright; see Terms of Use at http://library.seg.org/page/policies/terms
DOI:10.1190/1.3124936

anisotropy, and δ_b, ε_b are the Thomsen parameters of background sediment in the absence of stress perturbations. These expressions highlight that to a first degree seismic anisotropy is caused by differences between horizontal and vertical stresses in each vertical plane. It also underscores that overall anisotropy can be obtained by adding intrinsic and stress-induced contributions. Finally, the assumption of an isotropic third-order tensor with three independent constants leads to stress-induced anisotropy that is elliptic in nature. Indeed, one can see that stress-induced terms in Equations 4–5 are identical (in the weak-anisotropy limit) for δ and ε in the same symmetry plane, which is characteristic of elliptic anisotropy. Nevertheless total anisotropy remains nonelliptic ($\delta^{(1)}\neq\varepsilon^{(1)}$, $\delta^{(2)}\neq\varepsilon^{(2)}$) because intrinsic anisotropy is usually of a general character $\delta_b\neq\varepsilon_b$. Equations 4–5 are useful for understanding the impact of stress on reflection seismic signatures. For example, we can easily infer that azimuthal variation of P-wave NMO velocity is controlled by the difference between two horizontal principal stresses

$$\frac{V_{nmo}^{(1)}-V_{nmo}^{(2)}}{V_{nmo}^{(1)}}\approx\delta^{(1)}-\delta^{(2)}\approx\frac{K_p}{2C_{55}^0}(\sigma_{22}-\sigma_{11}) \qquad (6)$$

This equation contains a directly measurable seismic signature $V_{nmo}^{(1)}-V_{nmo}^{(2)}$. Therefore in the presence of reliable geomechanical information ($\sigma_{22}-\sigma_{11}$), we can directly invert at least for a single stress sensitivity parameter (c_{155}) from the azimuthal data.

Stress sensitivity parameters. To predict the changes in stiffness, we need three independent stress sensitivity parameters or nonlinear constants (c_{111}, c_{112}, and c_{123}) that can be obtained from:

1) laboratory measurement on cores under varying stress conditions
2) in-situ estimation using well logs, rock model, and geomechanical information
3) estimating coefficients between velocity and anisotropy perturbations and computed anomalous stress directly from wide-azimuth seismic data in areas where there is good illumination and sufficient signal

We initially used the laboratory estimate of stress sensitivity coefficients for a shale measurement interpreted by Prioul and Lebrat (2004): c_{111}= -7034, c_{112}= -2147, and c_{123}= 296 GPa. Field calibration with wide-azimuth data (Bachrach et al., 2007) using Equation 6 suggested that c_{155} needs to be scaled by a factor of 0.4, and so we scaled the remaining parameters by the same factor. We chose this parameter c_{155}= 489 GPa, so that it fits measured difference in azimuthal velocity computed with Equation 6. As an additional validation step, we compared it to other shale measurements interpreted by Prioul and Lebrat, and found that the coefficient value was reasonable.

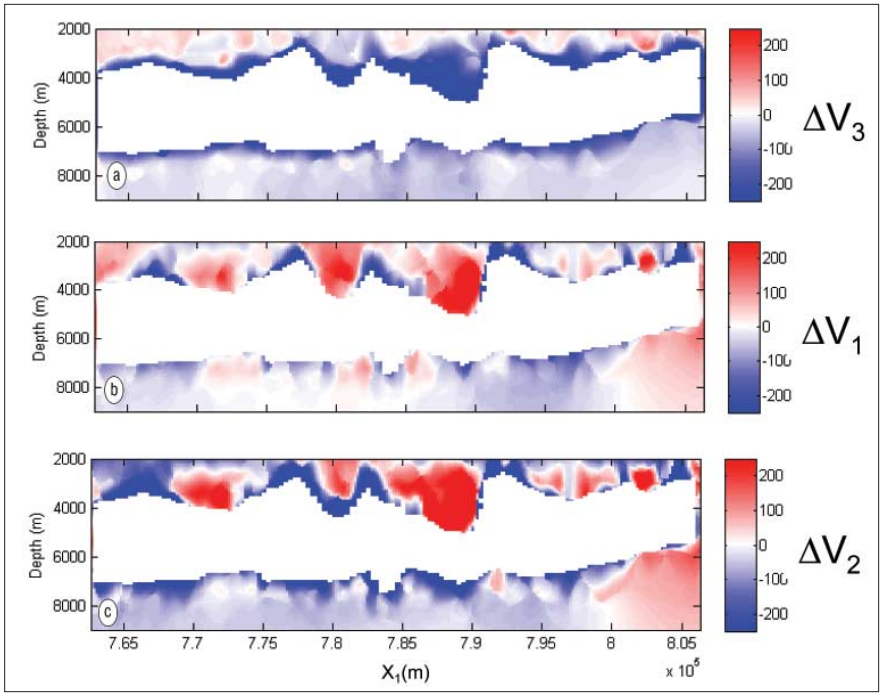

Figure 4. *Difference between updated and initial velocities shown as a cross section through the 3D model: (a) velocity change along vertical x_3-axis; (b) velocity change along horizontal x_1-axis; (c) velocity change along horizontal x_2-axis. They represent velocity perturbations caused by presence of salt bodies. Note the velocity reduction below salt and unequal values of two horizontal velocities, indicating azimuthal anisotropy.*

Results

Figure 4 shows 2D slices of the difference between the original and updated velocities in the vertical and two horizontal directions. For simplicity we assumed that sediment velocity in a reference state is isotropic $\delta_b=\varepsilon_b=\gamma_b=0$. Note the significant reduction in velocities (up to 250 m/s) below salt caused by geomechanical effects. Also observe that, in general, two horizontal velocities are different (compare Figure 4b and Figure 4c), which indicates azimuthal anisotropy caused by the unequal horizontal principal stresses. The magnitude of the velocity reduction is a function of the strain or stress magnitudes and the stress sensitivity coefficients. Using a different value of stress sensitivity coefficient will give a different estimate of velocity reduction; therefore, it is important to calibrate the result with available subsalt data.

To quantify the velocity variation for a range of angles around the vertical direction, it is instructive to visualize variation of orthorhombic parameters in a 2D section (Figure 5). We observe that stress-induced velocity anisotropy is quite pronounced and suggest that we can expect large spatial variations in the values of ε and δ in the presence of complex salt geometries. One can observe that low and high spots of anisotropy are controlled to a first order by differences between two principal stresses or strains (Equations 4 and 5 and Figure

Downloaded 01/02/23 to 73.136.105.228. Redistribution subject to SEG license or copyright; see Terms of Use at http://library.seg.org/page/policies/terms
DOI:10.1190/1.3124936

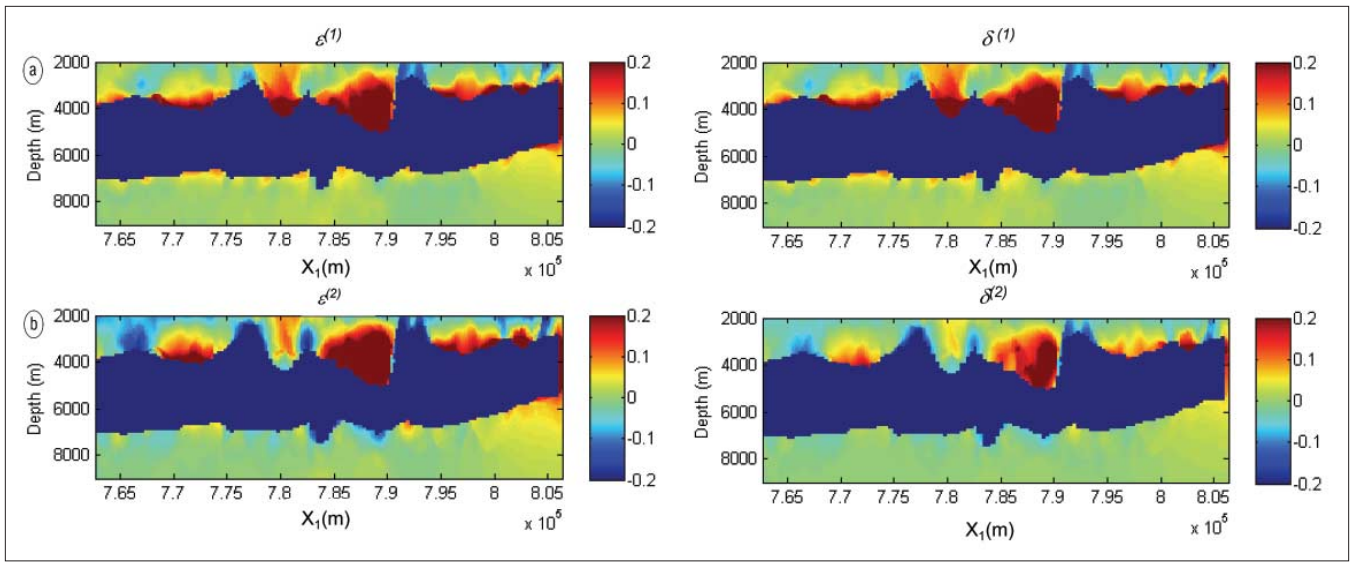

Figure 5. *Stress-induced anisotropy caused by presence of salt bodies is shown as anisotropic parameters of stressed orthorhombic media along the transect through the 3D model: (a) anisotropic parameters $\delta^{(1)}$, $\varepsilon^{(1)}$ that characterize polar anisotropy in the plane $[x_1,x_3]$ orthogonal to the cross section; (b) anisotropic parameters $\delta^{(2)},\varepsilon^{(2)}$ that characterize polar anisotropy in the plane $[x_1,x_3]$ parallel to the cross section. We observe significant differences between these two sets of parameters, thus indicating azimuthal anisotropy ($\delta^{(1)} \neq \delta^{(2)}$, $\varepsilon^{(1)} \neq \varepsilon^{(2)}$). We do not compute anisotropy values within the salt body. Observe "hot" spots of anisotropy caused by complex salt shape controlled by spatial variations of strain differences (Figure 3).*

3). Since variation of horizontal strains or stresses is different for two horizontal axes (Figures 3a and 3b), the anisotropic parameters in the two vertical symmetry planes remain generally unequal (Figures 5a and 5b). If a narrow-azimuth survey is conducted along the vertical symmetry plane x_2, x_3, then orthorhombic parameters $\delta^{(1)}$ and $\varepsilon^{(1)}$ are required to describe P-wave anisotropy caused by stresses. Likewise, for a narrow-azimuth survey along the x_1, x_3 plane, relevant orthorhombic parameters are $\delta^{(2)}$ and $\varepsilon^{(2)}$. If narrow-azimuth acquisition is performed in an arbitrary direction, then some effective VTI description can be found for this vertical symmetry place as described by Tsvankin which requires a combination of $\delta^{(1)}$, $\delta^{(2)}$, $\varepsilon^{(1)}$, $\varepsilon^{(2)}$. However, modern wide-azimuth marine surveys span a substantial range of azimuth. Geomechanical models coupled with a rock physics transform suggest that we may need azimuthally anisotropic P-wave velocity field in the vicinity of the salt bodies, in order to image wide-azimuth surveys. Salt geometry may also lead to the rotation of the stress field so that none of the principal stresses is vertical. In this case, velocity model resembles tilted orthorhombic or more general symmetry which is a subject of a separate study.

If one is unable to handle azimuthally anisotropic orthorhombic models in seismic processing, it makes sense to examine "averaged" azimuthally isotropic effects introduced by geomechanics. Figure 6 displays a 2D section of the P-wave VTI anisotropy parameters (with null values inside the salt body) computed by simple arithmetic averaging of corresponding orthorhombic parameters from Figure 6:

$$\delta_{avg} = \frac{\delta^{(1)} + \delta^{(2)}}{2}, \varepsilon_{avg} = \frac{\varepsilon^{(1)} + \varepsilon^{(2)}}{2}$$

They represent an average VTI representation of stress-induced

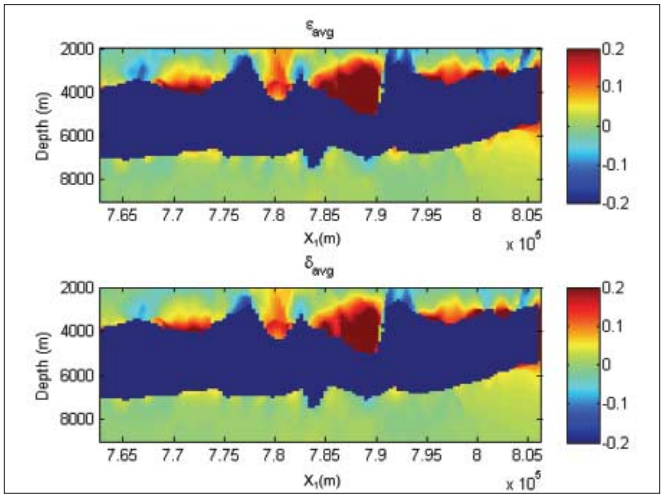

Figure 6. *Average VTI stress-induced anisotropy caused by presence of salt is quantified by Thomsen parameters shown along a 2D cross section through the 3D model. These VTI parameters are obtained by averaging orthorhombic parameters from Figure 5 and represent effective VTI anisotropy caused by anomalous salt-induced stresses.*

effects and underscore the substantial lateral variation of velocity and anisotropy around salt bodies that is currently not captured by tomographic algorithms above salt and unlikely to be ever captured below salt. Nevertheless, these variations may be crucial for correct imaging and target positioning near and below salt. Geomechanical modeling provides a good tool to delineate areas of high concentrations of anisotropy and, thus, can guide insertion of lateral variations of anisotropic parameters while building realistic velocity models consistent with geomechanics. At the very least, geomechanical model-

Downloaded 01/02/23 to 73.136.105.228. Redistribution subject to SEG license or copyright; see Terms of Use at http://library.seg.org/page/policies/terms
DOI:10.1190/1.3124936

ing makes us analyze velocity scenarios that are driven by geology and physics as opposed to ungeological and unphysical scanning of velocities in arbitrarily defined regions.

Discussion

We observe three important effects caused by the presence of a complex salt body. First, we can expect significant velocity reduction below large salt bodies as a consequence of the density contrast between the salt and sediments. Second, we observe spatially varying values of ε and δ, with the largest anisotropy occurring near the flanks of the salt body. Third, the ε and δ values are different in two orthogonal vertical planes, indicating that we can expect not only transversely isotropic, but also azimuthal anisotropy in the vicinity of salt bodies. An additional effect is related to rotation of principal stresses in the vicinity of the salt bodies. It is well known that around salt, the direction of largest principal stress substantially deviates from the vertical. The same observation applies to remaining principal stresses that may no longer lie in the horizontal plane. If principal stresses are rotated, then, strictly speaking, stress-induced anisotropy leads to a symmetry that is at least tilted orthorhombic, where symmetry planes or axes of effective anisotropic media are controlled by frame of the principal stresses.

Calibration of the results from geomechanical modeling is very important and can be done in several different ways. Ideally, we would have laboratory measurements of third-order elasticity coefficients on core samples. However, such measurements are scarce. Alternatively, stress sensitivity coefficients can be estimated from borehole acoustic. Another possibility is to estimate stress sensitivity coefficients from wide-azimuth seismic data in an area where the subsalt data quality is sufficiently robust. In our opinion, even with limited knowledge of the stress sensitivity coefficients, one can explore their effect given reasonable range of published parameters. Further research on the relationship between nonlinear parameters and the sedimentary column in different basins can facilitate such analysis.

Salt and sediments are not purely elastic. In general, geomechanical modeling of complex salt bodies should use a viscoelastic constitutive relationship for salt, and introduce perhaps elastoplastic behavior (and/or failure criteria) for surrounding sediments. Furthermore, pore pressure should be taken into account, and a poroelastic relationship should be used for detailed geomechanical modeling.

We demonstrate a workflow for using a simple geomechanical model to estimate improved velocity and anisotropy parameters around salt bodies. We recommend that for drilling applications and borehole stability analysis, a more detailed geomechanical model should be used as mentioned above.

Conclusions

We present a geomechanically constrained 3D modeling approach that combines stress-strain modeling with a rock physics transform to improve velocity and anisotropy estimates around salt bodies. Starting with an isotropic velocity model, we use geomechanical modeling to compute salt-induced stresses and strains around a large and complex salt geometry. The model takes into account the contrast in density and stiffness between salt and its surrounding sediments. Therefore, it can predict subsalt stress reduction (primarily caused by the density contrast and thickness), as well as stress anisotropy near the edges of the salt body (primarily caused by the salt geometry and contrast in stiffness). From salt-induced stresses and strains, we predict updates to the velocity model and anisotropy parameters using rock physics transform based on nonlinear elasticity. The updated velocity model improves upon simplistic depth trends or well-log interpolations, as it can predict subsalt velocity reduction as well as spatial variations in the anisotropic parameters. Updating velocity from geomechanics can be a powerful tool for imaging and pore-pressure prediction once it is calibrated with available subsalt data from wells as well as wide-azimuth seismic data.

Suggested reading. "Numerical modeling and observation from wide-azimuth marine data" by Bachrach et al. (EAGE 2007 *Extended Abstracts*). "Influence of horizontal and vertical stresses on V_P-V_S trends" by Bakulin et al. (SEG 2008 *Expanded Abstracts*). "Stress perturbations adjacent to salt bodies in the deepwater gulf of Mexico" by Fredrich et al. (SPE paper 84554, 2003). "Marine seismic surveys with enhanced azimuth coverage: Lessons in survey design and acquisition" by Howard (*TLE*, 2007). "Subsalt imaging: The RAZ-WAZ experience" by Kapoor et al. (*TLE*, 2007). "Nonlinear rock physics model for estimation of 3D subsurface stress in anisotropic formations: Theory and laboratory verification" by Prioul et al. (Geophysics, 2004). "Calibration of velocity-stress relationships under hydrostatic stress for their use under non-hydrostatic stress conditions" by Prioul and Lebrat (SEG 2004 *Expanded Abstracts*). "Anisotropic inversion of seismic data for stressed media: Theory and a physical modeling study on Berea sandstone" by Sarkar et al. (Geophysics, 2003). *Seismic Signatures and Analysis of Reflection Data in Anisotropic Media* by Tsvankin (Elsevier, 2005). TLE

Acknowledgments: We acknowledge BHP Billiton Petroleum for valuable discussions. We thank Michael O'Briain and Ilgar Atakishiyev of WesternGeco for providing the salt geometry.

Corresponding author: msengupta@slb.com